

## DIRECTIONS IN SECONDARY LITHIUM BATTERY RESEARCH AND DEVELOPMENT

K. M. ABRAHAM

EIC Laboratories Inc., 111 Downey Street, Norwood, MA 02062, U.S.A.

(Received 15 September 1992)

**Abstract**—The diverse directions in which research and development on ambient temperature secondary lithium batteries is proceeding are discussed. The state-of-the-art in liquid electrolyte-based systems containing Li metal as the anode can be described in terms of the various AA-size cells developed; they are capable of 250–300 full depth of discharge cycles, specific energies of 100–130 Wh kg<sup>-1</sup> and energy densities of 250–300 Wh l<sup>-1</sup>. The commercialization of these batteries has been deterred by concerns of safety hazards. Approaches being pursued to resolve the safety issue include the identification of new or improved electrolytes, the use of alternative anodes, such as lithiated carbon with lower Li activity, and improved microporous separators having smaller pore size, higher porosity and “shut down” capability. The emergence of the carbon anode-based “Li ion” batteries as potentially safe systems makes it necessary to identify organic electrolytes with oxidative stability to potentials of up to 5V vs. Li<sup>+</sup>/Li. Solid-polymer electrolyte-based solid-state batteries are being developed for a variety of military and consumer applications including electric vehicle propulsion. Solid-state batteries with performance reminiscent of their liquid electrolyte counterparts can be fabricated with the use of non-conventional polymer electrolytes. These are composed of low volatility organic liquid electrolytes embedded in organic polymer networks and have conductivities of >10<sup>-3</sup> ohm<sup>-1</sup> cm<sup>-1</sup> at 20°C. A C/LiMn<sub>2</sub>O<sub>4</sub> cell utilizing such an electrolyte exceeded four hundred discharge/charge cycles.

*Key words:* lithium, secondary battery, liquid electrolytes, polymer electrolytes, insertion electrodes.

### INTRODUCTION

The last decade has seen significant advances in the ambient temperature Li battery technology; the development[1–5] and commercialization[5] of AA size cells with Li metal anodes, the commercialization of a low rate Li/MnO<sub>2</sub> coin cell for computer memory protection by Sanyo, the fabrication and testing of large Li cells ranging in capacities from 2 to 100 Ah for potential consumer and military applications[1, 6–10], the development and market-testing of a Li ion battery with lithiated carbon anode by Sony[11], and the development of polymer electrolytes with conductivities approaching those of liquid electrolytes[12–14]. These achievements are nothing short of spectacular when it is considered that until the late seventies ambient temperature secondary lithium batteries were a mere laboratory curiosity. The extraordinary emphasis currently given to secondary Li batteries can be traced to a need for reliable, high energy, high power, rechargeable batteries for use in portable equipment such as telephones, televisions, video cameras, computers and electric vehicle propulsion. Batteries with specific energies of 100–150 Wh kg<sup>-1</sup>, energy densities of 250–300 Wh l<sup>-1</sup> and a specific power of greater than 100 W kg<sup>-1</sup> are desirable for these applications. In the following sections an attempt is made to discuss key issues in the various battery systems with the hope of bringing into focus present and future directions of research and development in the ambient temperature secondary lithium battery technology. It is to be noted that because of the complex nature of the subject matter[15], no attempt is made here to

present a comprehensive account of the world-wide efforts in secondary Li batteries; rather, it is an account biased by the experiences of the author. The other articles in this volume will certainly cover several of the areas in greater detail.

### LIQUID ELECTROLYTE-BASED SECONDARY LITHIUM BATTERIES

The data presented in Table 1 is a fair summary of the state-of-the-art of the technology based on the Li metal anode. The Li cells have specific energies between 100–130 Wh kg<sup>-1</sup> and energy densities up to 300 Wh l<sup>-1</sup>. In 10–100 Ah cells, values of up to 20 per cent greater than those given in Table 1 can be expected. The most important point is that some of the Li cells are capable of 3–4 times longer service life than the Ni/Cd cell. The Li cells have also demonstrated long cycle-life; for example, in the Li/TiS<sub>2</sub> cell we have obtained 200–300 cycles at full depth-of-discharge[2] and up to 1000 cycles at 50 per cent depth-of-discharge. The Ragone plots given in Fig.1 for the Ni/Cd and Li/TiS<sub>2</sub> cells illustrate the superior capabilities of the Li systems. Only at very high power densities of >500 W l<sup>-1</sup> will the Li system's performance become inferior to that of Ni/Cd. The reason for this divergence at high power is the poor conductivity of non-aqueous electrolytes compared to that of aqueous KOH. In light of these very attractive features of the Li systems, it will be asked, why are there not AA size Li secondary cells in commercial use today. The answer is safety hazards. This brings us to the foremost issue; safety

Table 1. Comparison of AA size ambient temperature secondary Li cells with the Ni/Cd cell

System	Capacity (mAh)	Voltage (V)	Wh Cell <sup>-1</sup>	Wh Kg <sup>-1</sup>	Wh l <sup>-1</sup>	Cycle life
New NiCd	850	1.2	1.02	45	130	> 500
Li/MoS <sub>2</sub>	600	1.8	1.08	54	140	> 300
Li/TiS <sub>2</sub> *	1050	2.15	2.25	130	290	> 300
Li/NbSe <sub>3</sub>	1100	1.95	2.15	90	265	> 200
Li/MnO <sub>2</sub>	700	2.8	1.96	115	240	> 200
Li/CuCl <sub>2</sub> /SO <sub>2</sub>	500	3.4	1.76	95	210	> 100
Li/SO <sub>2</sub>	550	3.0	1.65	90	200	> 100

\* Recent EIC Li/TiS<sub>2</sub> AA size cells (the ReLi<sup>®</sup> cell).

hazards of secondary cells containing Li metal anodes. A good understanding of the problem and appropriate solutions are prerequisites for the full acceptance of Li metal anode technology by consumers.

#### Safety hazards of secondary lithium batteries

At the root of the problem is the reactivity of elemental Li. From a thermodynamic stand-point, Li will react with all materials, inorganic as well as organic, and the stability Li enjoys in Li batteries is conferred by the passivation film (often referred to as the solid electrolyte interphase, SEI) formed on the Li surface from its reactions with the electrolyte. This stability has enabled the successful commercialization of a number of Li primary systems. In the early phases of the development of secondary Li cells, there was general optimism that any safety problems that arose would be solved quickly. This optimism appeared to be justified by the success in addressing analogous problems with primary Li cells and by the belief that electrolytes used in secondary cells were much less aggressive than those in the primary cells such as Li/SOCl<sub>2</sub> and Li/SO<sub>2</sub>.

However, the accumulated experience of the last few years has shown that safety problems with secondary Li cells are much more difficult than anticipated. The fundamental reason for this is the progressive formation of finely dispersed and, hence, highly reactive Li in a cell as it is repeatedly discharged and charged. This is quite different from the situation in primary Li cells where Li metal is consumed during discharge, and at the end of its useful discharge life there will usually be little or no elemental Li. In a secondary Li cell, on the other hand, Li metal is replated on the anode during charging[15]. Some of this Li reacts with the electrolyte, becomes passivated and permanently isolated from the bulk anode as finely divided Li. This phenomenon is common to all secondary Li cells and is more or less independent of the nature of the cathode.

Finely dispersed Li does not cause a cell to be unstable as long as the Li is passivated by the electrolyte. In fact, such is the case with all secondary Li cells under ordinary circumstances. However, if a cell is abused, particularly if its temperature is raised above the melting point of Li, either locally or globally within the cell, passivity is lost and the cell can vent, almost always with flame. The temperature in a cell can be raised by electrical abuse, *eg* internal or external shorts and overcharge. Experience suggests that an external short will lead to venting only if the temperature of the cell rises above 180°C, the melting point of Li. Internal shorts are a potential source of safety problems. Since Li is plated from a liquid electrolyte, there is always the possibility that a cell may develop a short, via "Li dendrites", between the anode and the cathode. Usually, such shorts are manifested by significantly longer charge inputs than the discharge and are called "soft-shorts" since they often disappear during discharge and the cell does not fail catastrophically. However, the short can conduct substantial currents and may cause significant local heating. The hot spot may melt the separator, exothermically decompose the electrolyte[16] or melt the Li. If the separator melts, the soft-short can become a "hard-short" with catastrophic cell failure. Even if the separator does not melt, the hot spot developed as a result of the soft-short can decompose the electrolyte which in the case of LiAsF<sub>6</sub>-containing electrolytes, such as ethylene carbonate (EC)/propylene carbonate (PC)-LiAsF<sub>6</sub>, and tetrahydrofuran (THF)/2-methyl-tetrahydrofuran (2Me-THF)/2-methyl-furan (2Me-F)-LiAsF<sub>6</sub>, can generate heat[16], can become self-sustaining through involvement of finely

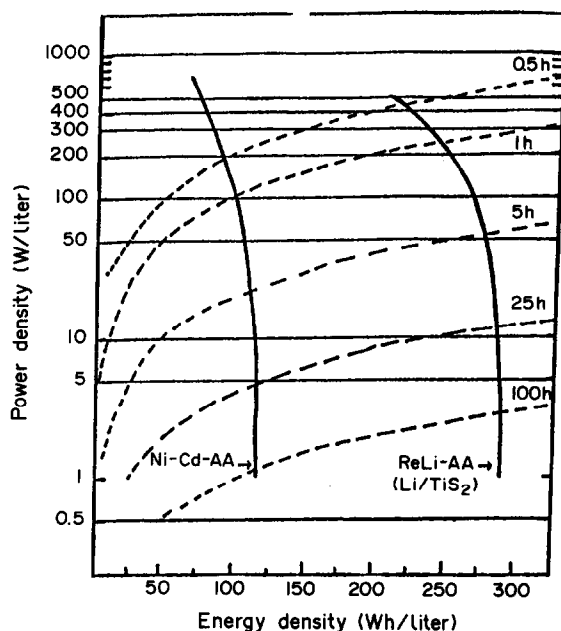


Fig. 1. Comparison of secondary Li/TiS<sub>2</sub> and Ni/Cd cells. The Li cell is the ReLi<sup>®</sup> cell manufactured by EIC.

divided Li and assist the venting reaction. If the local heating from internal shorts exceeds 180°C, Li will melt and a runaway reaction involving the finely dispersed Li and the electrolyte can occur.

We have found that internal shorts in small cells of sizes of 1 Ah or less are usually benign while such a condition in large cells of 10–100 Ah capacity can lead to catastrophic failure involving “venting with flame”. It appears that whether or not an internal short will generate sufficient heat locally depends on the amount of current it conducts which in turn is a function of the electrode size. The 1 Ah AA size cells appear to be borderline in their response to internal short; they have almost always shown safe behavior. One condition under which a 1 Ah cell may vent is when a cycled cell is heated. We have found that, almost always, 1 Ah Li/TiS<sub>2</sub> cell will vent with flame if it is heated to about 150°C after cycling a few times. Two events appear to occur at this temperature; the melting of the porous, polypropylene, separator membrane (Celgard 2400) and exothermic reactions of the electrolyte. These events may help increase the local cell temperature to or above the melting point of Li and initiate a run-away reaction. The electrolyte in EIC's Li/TiS<sub>2</sub> cell is a solution of LiAsF<sub>6</sub> in a mixture of tetrahydrofuran (THF), 2-methyl-tetrahydrofuran (2Me-THF) and 2-methyl-furan (2Me-F)[17].

The Li salts used for preparing nonaqueous electrolyte solutions are based on large anions[18], *eg* AsF<sub>6</sub><sup>-</sup>, PF<sub>6</sub><sup>-</sup>, CF<sub>3</sub>SO<sub>3</sub><sup>-</sup>, BF<sub>4</sub><sup>-</sup> and N(SO<sub>2</sub>CF<sub>3</sub>)<sub>2</sub><sup>-</sup>. These salts are reducible by Li as illustrated in equation (1) for LiAsF<sub>6</sub>.



The reaction shown in equation (1) will generate about 390 kcal of heat which, under adiabatic conditions can raise the temperature of a AA size cell to about 600°C. Obviously, this reaction does not take place under the normal cycling of cells because of the kinetic stability of Li from passivating surface films. In all likelihood, the passivating film on Li is composed of LiF along with products of chemical and electrochemical reactions involving the solvent and the Li salt[19]. Once the Li has lost its passivity, for example by local heating, an exothermic reaction can be initiated and can become self-sustaining because of the large amount of heat involved. The irony is that the use of LiAsF<sub>6</sub> as a salt is apparently essential for high efficiency cycling of the Li electrode in organic media such as the solvent mixtures of THF/2Me-THF[17], EC/PC[20], EC/PC/triglyme[21] and 2Me-THF/EC[22]. It is clear that the identification and characterization of electrolytic solutions is an important area of research in the development of safe secondary Li batteries. Ideally, the Li salt would be stable to reductive reaction with Li, and the Li salt, and the solvent would be compatible and will not decompose when heated up to 180°C.

In searching for electrolytic solutions for safe secondary Li batteries a number of factors must be considered. Generally, organic solvents having large dipole moments and high dielectric constants dissolve appreciable amounts of Li salts. Dissolution of a Li salt in a solvent occurs when the solvation energy (the heat of complexation of the solvent by

the Li salt) exceeds the lattice energy of the salt. The dissolved salts are substantially associated. It is also desirable to have low viscosities for the solvents in order to maintain high ionic mobility, and consequently, high conductivity at low temperatures; for example 0 to -40°C. Note that ambient temperature batteries must perform well over the -40 to 70°C range. As far as Li salts are concerned, those having large anions with low lattice energies provide the most conductive solutions. The conductivities of a series of Li salts in tetrahydrofuran are listed in Table 2. While THF-Li-SbF<sub>6</sub> and THF-LiAlCl<sub>4</sub> solutions exhibit high conductivities, Li cannot be plated from these solutions since the favored reaction appears to be the reduction of Sb<sup>V</sup> or Al<sup>III</sup>. Conversely, the highly conductive THF-LiAsF<sub>6</sub> solution does allow high-rate plating and stripping of Li. This advantage of THF-LiAsF<sub>6</sub> solutions over those containing LiAlCl<sub>4</sub> and LiSbF<sub>6</sub> may be attributed to the properties of the passivating film (SEI) that form on Li in presence of LiAsF<sub>6</sub>. This film, while permeable to Li<sup>+</sup>, is apparently impermeable to AsF<sub>6</sub><sup>-</sup>. The films formed in LiSbF<sub>6</sub> and LiAlCl<sub>4</sub> containing solutions do not seem to have this selectivity. The conductivity of the THF-LiClO<sub>4</sub> solution is low. It should also be remembered that LiClO<sub>4</sub> is incompatible with ethers in general and that has been the reason for abandoning the dioxolane-LiClO<sub>4</sub> solutions although Li was cycled with high efficiency in it[23].

The need for new electrolytes, particularly Li salts, from the perspective of safe secondary Li batteries has been recognized and new salts such as lithium bis(trifluoromethane sulfone)imide, LiN(SO<sub>2</sub>CF<sub>3</sub>)<sub>2</sub>, and tris(trifluoromethane sulfone) methide, LiC(SO<sub>2</sub>CF<sub>3</sub>)<sub>3</sub>, have been synthesized[24]. These salts do form highly conductive solutions in THF, EC and PC. Conductivities of THF-LiN(SO<sub>2</sub>CF<sub>3</sub>)<sub>2</sub> (1M) and 1:1 EC:PC-LiN(SO<sub>2</sub>CF<sub>3</sub>)<sub>2</sub> (1M) are  $9 \times 10^{-3}$  and  $5 \times 10^{-3}$  ohm<sup>-1</sup> cm<sup>-1</sup>, respectively, at room temperature. From a cell safety standpoint, however, these salts do not appear to be fully satisfactory. This is because they do contain fluorine atoms which can react exothermically with Li generating almost the same amount of heat as LiAsF<sub>6</sub>. In fact, our preliminary experiments indicated that AA size Li/TiS<sub>2</sub> cells containing the THF/2Me-THF-LiN(SO<sub>2</sub>CF<sub>3</sub>)<sub>2</sub> electrolyte would vent with flame when heated to about 140°C after cycling a few times. Thus, the safety-related behavior of these cells appeared not to be any different from that of cells containing the THF/2Me-THF-LiAsF<sub>6</sub> electrolyte.

Research aimed at safe secondary Li cells emphasizes in addition to new liquid electrolytes: (i)

Table 2. Conductivities of Li salts in tetrahydrofuran

Electrolyte	Conductivity (ohm <sup>-1</sup> cm <sup>-1</sup> )
THF/LiSbF <sub>6</sub> (1 M)	$16 \times 10^{-3}$
THF/LiAlCl <sub>4</sub> (1 M)	$16 \times 10^{-3}$
THF/LiAsF <sub>6</sub> (1 M)	$14 \times 10^{-3}$
THF/LiClO <sub>4</sub> (M)	$3.3 \times 10^{-3}$
THF/LiBF <sub>4</sub> (1 M)	$1.7 \times 10^{-3}$
THF/LiBr (1 M)	$5 \times 10^{-5}$

approaches to increase the Li anode cycling efficiency including the use of additives to the electrolyte[17]; (ii) improved separators particularly those with "shutdown properties"; and (iii) alternative anodes such as Li-alloys, Li insertion compounds and carbon. Some of these topics are addressed below:

#### High-efficiency cycling of the Li electrode

It is possible to plate Li with 100% efficiency in most organic electrolyte solutions; but it cannot be electrochemically stripped as efficiently[18]. As already mentioned, a fraction of the Li plated (recharged) on to a substrate from solution becomes electrically isolated due to passivation by products of its reaction with the electrolyte or impurities in the electrolyte. Consequently, less Li is stripped (discharged). That is,

$$\text{Li cycling efficiency, } E_{\text{Li}} = \frac{Q_s}{Q_p} \times 100 = < 100\%. \quad (2)$$

The principal goal of research on Li anode rechargeability is to bring the ratio of Li stripped ( $Q_s$ ) to Li plated ( $Q_p$ ) as close to 100 per cent as possible. The relationship between Li cycling efficiency and cell cycle-life can be illustrated as follows. A convenient way of expressing Li cycling efficiency is in terms of the Figure of Merit,  $\text{FOM}_{\text{Li}}$  or Li turnover number.

$$\text{FOM}_{\text{Li}} = \left( \frac{1}{1 - \frac{E}{100}} \right) = N \frac{Q_d}{Q_i} \quad (3)$$

In equation (3),  $N$  is the total number of cycles,  $Q_d$  is the capacity in each discharge and  $Q_i$  is the capacity initially present in the cell. Typically, rechargeable Li cells utilize an initial Li capacity of about three times as much as the cathode. (Higher amounts will severely decrease the energy density of the cell). That means that in a practical cell  $Q_i$  is about  $3Q_d$ . Therefore, the  $\text{FOM}_{\text{Li}}$  required for 1000 cycles is

$$\text{FOM}_{\text{Li}} = \frac{1000Q_d}{3Q_d} = 333.3 \quad (4)$$

That is to say that the Li anode must cycle with an efficiency of 99.7%, a tall order indeed. To date, efficiencies up to about 99%, or a  $\text{FOM}_{\text{Li}}$  of  $\sim 100$ , have been demonstrated[2].

The conventional wisdom is that the cycling efficiency of the Li anode is intimately connected with the reactivity of the electrolyte with Li; the lower this reactivity, the greater is the cycling efficiency. It was found, for example, that when Li was cycled in PC based electrolyte, the freshly plated Li was passivated so much by  $\text{Li}_2\text{CO}_3$ , the product of the reaction between PC and Li, that extremely low Li cycling efficiencies were obtained[18]. Following these early observations, organic electrolyte solutions were sought in which the reactivity of the organic solvents towards Li was abated by modification of the electronic properties of the solvents. Thus, better Li cycling was achieved in 2Me-THF-LiAsF<sub>6</sub> than in THF-LiAsF<sub>6</sub>[18]. Although this approach of modifying the electronic properties of the solvents appears useful and can lead to useful solvents, recent data suggest that high efficiency Li cycling in secondary Li batteries is the result of a combination of factors, *eg*: low reactivity of Li with the solvent and the salt; high conductivity of the electrolyte solution; an optimum electrode stack pressure in cell to achieve high density Li plates during charging; additives to form a favorable Li surface passivation film (SEI); charging current density and method of charging; and possibly other factors not yet identified. The following examples illustrate the importance of some of these.

The very low Li cycling efficiency in THF-LiAsF<sub>6</sub> ( $\text{FOM}_{\text{Li}} = 2.2$ ), despite the high conductivity of the solution, can be attributed to the high reactivity of Li with THF[17]. On the other hand, a significantly higher Li cycling efficiency is obtained in 2Me-THF-LiAsF<sub>6</sub> ( $\text{FOM}_{\text{Li}} = 16$ ) although the conductivity of this solution is about four times lower than that of the THF solution. Evidently, the kinetic stability of 2Me-THF towards Li is better than that of THF. A disadvantage of rechargeable Li cells utilizing 2Me-THF-LiAsF<sub>6</sub> solutions, however, is that they behave poorly at low temperatures,  $eg \leq -10^\circ\text{C}$ . This has been attributed to the crystallization of solvates of LiAsF<sub>6</sub> at these temperatures. Improved low temperature performance can be achieved with mixed ether solutions such as a mixture of THF and 2Me-THF-containing LiAsF<sub>6</sub>. A key discovery in this connection was the aforementioned 2Me-Furan as an additive to obtain significantly higher cycling efficiency in THF-containing solutions[17] (Table 3).

The data presented in Table 3 were obtained in laboratory test cells with flooded levels of electrolyte. In AA size Li/TiS<sub>2</sub> cells with a significantly lower

Table 3. Lithium cycling in tetrahydrofuran solutions with and without 2-Methylfuran (obtained in lab cells with flooded level of electrolyte)

Electrolyte	Vol.% 2-MeFuran	Number of cycles in a Li/TiS <sub>2</sub> cell	Li cycling efficiency ( $\text{FOM}_{\text{Li}}$ )
THF/LiAsF <sub>6</sub> (1.5 M)	0	7	2.2
THF/LiAsF <sub>6</sub> (1.5 M)	0.5	110	19
2Me-THF/LiAsF <sub>6</sub> (1.5 M)	0	95	16
2Me-THF/LiAsF <sub>6</sub> (1.5 M)	0.5	185	33
1:1 THF:2Me-THF/LiAsF <sub>6</sub> (1.5 M)	0	51	8
1:1 THF:2Me-THF/LiAsF <sub>6</sub> (1.5 M)	0.5	145	25

electrolyte to electrode ratio, on the other hand, we obtained a Li cycling efficiency of about 99% ( $FOM_{Li} = \sim 100$ ) when the electrolyte was 1:1 THF/2Me-THF-LiAsF<sub>6</sub> (1.5 M) with about 4 v/o 2Me-F. This significantly higher cycling efficiency consistently obtained in the AA size cells, with spirally wound electrodes, in comparison to that obtained in laboratory cells can be attributed to the greater electrode stack pressure in AA size cells leading to better morphology for the plated Li and the resulting lower reactivity and less loss of Li per cycle. The advantage of an optimum electrode stack pressure for obtaining high Li cycling efficiency was experimentally verified in Li/MoS<sub>2</sub> rechargeable cells containing the EC/PC-LiAsF<sub>6</sub> electrolyte[25]. We, however, found that AA size Li/TiS<sub>2</sub> cells exhibited shorter cycle life when the electrolyte was 2Me-THF-LiAsF<sub>6</sub> (1.5 M) with 2Me-F, despite the fact that this electrolyte led to the best performance of lab cells. This disparate cycle life behavior of the two types of cells can be attributed to the interplay of cell impedance and the Li to electrolyte reactivity. Reactions between Li and the electrolyte consume the electrolyte during cell cycling and increase the cell's impedance[7]. We have found that this occurs with both 2Me-THF-LiAsF<sub>6</sub> and THF/2Me-THF-LiAsF<sub>6</sub>. However, since the latter electrolyte is twice as conductive as 2Me-THF-LiAsF<sub>6</sub> to start with, the impedance in cells containing the mixed electrolyte remains significantly lower for the same rate of salt consumption with cycling. Thus, because of its lower conductivity the 2Me-THF-LiAsF<sub>6</sub> solution gives rise to shorter cycle life in AA size Li/TiS<sub>2</sub> cells although chemically this solution is the most stable towards Li. Recently, it has been reported that the cycle life of AA size Li/TiS<sub>2</sub> cells containing 2Me-THF-LiAsF<sub>6</sub> can be increased with the addition of about 10 volume per cent EC[26]. It is interesting that the conductivity of 2Me-THF-LiAsF<sub>6</sub> (1 M) increases from about  $3 \times 10^{-3} \text{ ohm}^{-1} \text{ cm}^{-1}$  at 20°C to about  $10^{-2} \text{ ohm}^{-1} \text{ cm}^{-1}$  with the addition of about 50 v/o EC[27]. Consequently, a 10 per cent EC will probably result in at least a fifty per cent increase in the conductivity of 2Me-THF-LiAsF<sub>6</sub> (1.5 M) and that could explain the longer cycle life of the EC containing cells.

Ethylene carbonate probably also modifies the surface film (SEI) on the Li anode so as to result in a more favorable morphology for the Li being plated from solution. This is exemplified not only by the aforementioned results in 2Me-THF/EC-LiAsF<sub>6</sub> electrolytes but also by the long cycle life of Li/MoS<sub>2</sub> and Li/MnO<sub>2</sub> cells containing EC/PC-LiAsF<sub>6</sub>[5] and Li/NbSe<sub>3</sub> cells with EC/PC/triglyme-LiAsF<sub>6</sub>[3]. It should also be noted that the addition of CO<sub>2</sub> to methylformate based electrolyte solutions apparently increases cycle life of Li/LiCoO<sub>2</sub> cells[28].

The nature of the Li surface films formed in solutions containing 2Me-F, CO<sub>2</sub>, or EC have not yet been well characterized and this remains an important area of future research. Our own work has shown that 2Me-F is consumed during cell cycling[17, 29]. Others have found lower Li/electrolyte interfacial impedance in presence of 2Me-F[30], and cells containing 2Me-F in the electrolyte

generated lower amounts of heat of corrosion of Li than those without 2Me-F[31]. However, much further work remains to be done in understanding the behavior of the Li-electrolyte interface. Exploring the physical and chemical properties of Li surface films (SEI) is an important area of future research, relevant to cell safety and cycle life.

It is recognized that high Li cycling efficiencies are obtained at low charge current densities ( $\leq 0.5 \text{ mA cm}^{-2}$ ) and low depths of charge ( $2\text{--}3 \text{ mAh cm}^{-2}$ ). This can be attributed to the interplay of Li morphology and cycling efficiency, a good morphology being favored by a low current density and a low depth of charge. Irregular Li morphologies and dendrites are encouraged by high current densities and non-homogeneous current distribution. One of the cell components that probably affects Li plating morphology and encourages dendrite growth is the separator in the battery. The microporous separators used in secondary Li batteries have a porosity of only about 35%. It is conceivable that with such low porosity separators, low current densities have to be used for homogeneous current distribution over the Li electrode, whose 65% geometric area is facing solid portions of the separator, and suppression of Li dendrite growth. The role of separator properties on Li cycling has not yet been systematically dealt with, but may be of importance in realizing a safe, reliable, long cycle life battery.

## SEPARATORS IN SECONDARY LITHIUM BATTERIES

Polypropylene or polyethylene microporous flat sheet membranes are used as separators to electronically isolate the negative and positive electrodes in secondary Li batteries[32]. These materials are chemically and electrochemically stable in secondary Li batteries containing a wide variety of metal oxide and sulfide cathode materials. The ionic resistivity of the porous membrane is essentially the resistivity of the electrolyte that is embedded in the pores of the separator. It is a function of the membrane's porosity, tortuosity of the pores, the resistivity of the electrolyte, the thickness of the membrane and the extent to which the electrolyte wets the pores of the membrane. The ratio of the resistivity of a separator membrane to that of the electrolyte is called McMillin Number,  $N_M$ , which can be used to predict the influence of the separator on battery performance[33], *eg* voltage loss due to *IR* drop across the separator and ionic mass transport in the battery. A key requirement of separators for Li anode batteries is that their pores be small enough to prevent dendritic Li penetration through them. On the other hand, as mentioned earlier, a low separator porosity can be a factor that encourages dendrite formation because of nonhomogeneous current distribution. Dendritic Li growth through a separator can also probably be suppressed with a relatively high tortuosity of the pores although the resistivity of the separator will increase with increasingly tortuosity. Recently we have determined the resistivity and tortuosity of a number of Celgard

membranes[34]. It is pertinent to discuss the results of that study here.

First of all we developed a method for experimentally determining the resistivity of microporous separators. The resistivity was determined by the *ac* method since *dc* can polarize the electrode and cause electrolysis of the solution. The tortuosity and McMullin numbers were calculated from the resistivity data for a number of Celgard separators. The resistivities of separator membranes were determined by a difference method. First, the resistance ( $R_1$ ) of an electrochemical resistivity cell (hereafter referred to as the ER cell) containing a non-aqueous electrolyte was determined. The Celgard membrane was then placed between the two electrodes of the ER cell and the resistance of the cell ( $R_2$ ) was again measured.

The measured resistance of the ER cell without the separator,  $R_1$ , can be expressed as

$$R_1 = \rho_s K \quad (5)$$

where  $\rho_s$  is the specific resistance (ohm cm) of the electrolyte, commonly called the resistivity, and  $K$  ( $\text{cm}^{-1}$ ) is cell constant determined by calibration with an aqueous KCl solution. The resistance of the cell with separator,  $R_2$ , can be written as

$$R_2 = R_1 + R_m - \rho_s l_m / A_m \quad (6)$$

$R_m$  symbolizes the resistance of the membrane saturated with the electrolyte and the last term in the right hand side of equation (6) represents the displacement of the electrolyte by the separator, where  $l_m$  is the thickness of the Celgard membrane and  $A_m$  is its cross-sectional geometric area. By combining equations (5) and (6), the resistivity (ohm cm) of the Celgard membrane saturated with the electrolyte,  $\rho_m$ , can be calculated. That is,

$$R_m = (R_2 - R_1) + \rho_s l_m / A_m \quad (7)$$

But,

$$R_m = \rho_m \frac{l_m}{A_m} \quad (8)$$

Therefore,

$$\rho_m = (R_2 - R_1) A_m / l_m + \rho_s \quad (9)$$

$\rho_m$  is essentially the resistance of a 1 cm thick membrane saturated with the electrolyte having a cross-section geometric area of 1  $\text{cm}^2$ . Alternatively, it is the resistance between opposite faces of a 1 cm cube of the membrane saturated with the electrolyte.

The area-specific resistivity of a membrane,  $\rho_{ma}$ , (ohm  $\text{cm}^2$ ), is calculated by multiplying  $\rho_m$  (ohm cm) by the thickness of the membrane,  $l_m$ . That is,

$$\begin{aligned} \rho_{ma} &= (R_2 - R_1) \frac{A_m}{l_m} l_m + \rho_s l_m \\ &= (R_2 - R_1) A_m + \rho_s l_m \end{aligned} \quad (10)$$

The McMullin number,  $N_m$ , is the ratio of the resistivity of the film to the resistivity of the electrolyte

$$N_m = \frac{\rho_m}{\rho_s} = (R_2 - R_1) \frac{A_m}{l_m \rho_s} + 1 \quad (11)$$

Using  $N_m$  together with the porosity ( $P$ ) of the membrane, the tortuosity factor  $T$  can be derived as follows.

Celgard membranes are insulators and, consequently, the conductive part of the membrane is the electrolyte within the free volume of the membrane. Then, the resistance of the membrane  $R_m$  can be expressed by the specific resistivity of the electrolyte  $\rho_s$  and the tortuosity  $T$  and the porosity  $P$ , of the membrane. That is,

$$R_m = \rho_s \frac{T l_m}{P A_m} = \rho_s \frac{T^2 l_m}{P A_m} \quad (12)$$

But, the specific resistivity of the membrane is given by equation (8).

Dividing equation (8) by (12) and from the definition of the McMullin number, we have

$$N_m = \frac{\rho_m}{\rho_s} = \frac{T^2}{P} \quad (13)$$

That is, the tortuosity is given by

$$T = \sqrt{N_m P} \quad (14)$$

The resistivity, tortuosity and McMullin number for a number of membranes are listed in Tables 4 and 5.

The availability of these data makes it now possible to assess the influence of the separator on Li

Table 4. Resistivity of Celgard membranes measured in THF/1.5 M LiAsF<sub>6</sub>

Celgard® membrane	% Porosity	Resistivity ( $\Omega \text{cm}^2$ )	$N_m$	$T$
2400	32	3.1	23	2.7
2402	32	6.15	22	2.8
K-256	36	2.6	10	1.9
K-273	39	0.7	4	1.2
4400	34	6.8	43	3.8
4410	36	4.8	28	3.2
2500	42	3.8	23	3.2
4500	41	1.6	10	2.0
4525	43	7.0	42	4.3
4560	44	8.8	54	4.9
K-864	60	0.3	1.2	0.9
K-871	32	9.5	68	4.7
K-878	55	6.4	53	5.3
K-881	33	1.6	10	1.9
K-203	37	1.4	16	2.4

\* Thickness of the membranes vary between 25 and 50  $\mu\text{m}$ .

Table 5. Resistivity of Celgard membranes measured in PC/1.0 M LiAsF<sub>6</sub>

Celgard® membrane	% Porosity	Resistivity ( $\Omega \text{cm}^2$ )	$N_m$	$T$
3400	34	21.8	45	3.9
3401	38	11.6	23	3.0
3402	37	6.5	13	2.2
3406	37	10.7	21	2.8
D-552	44	7.4	15	2.6
D-511	43	4.9	10	2.1

battery performance. For example, the primary contribution to the ohmic resistance,  $R_{cell}$  in most Li batteries is the resistivity of the separator saturated with electrolyte. Knowing the latter, the expected cell resistance can be calculated. That is,

$$R_{cell} = \frac{\rho_{ma}}{A}, \quad (15)$$

where  $A$  is the area of the separator facing the electrodes. In this way, quick decisions can be made regarding the usefulness of a separator for a given application.

We have evaluated the performance of AA size Li/TiS<sub>2</sub> cells with five different Celgard membranes; 2400, 2402, 2500, K-273 and K-878. The cells were a shorter version of the ones described in [2]. The discharge curves obtained at 4 mA cm<sup>-2</sup> are presented in Fig. 2. Discharge/charge cycling data obtained from these cells led us to conclude that Celgard 2400, 2402 and K-273 are the most desirable separators among the five membranes. The cycling curves for a AA size Li/TiS<sub>2</sub> cell containing Celgard 2400 are presented in Fig. 3. The pore sizes of these membranes are given in Table 6. Celgard 2402 is a double laminated version of Celgard 2400; they have a

Table 6. Pore sizes in some Celgard membranes

Celgard® membrane	Pore size (μm)
2400	0.05 × 0.125
2402	0.05 × 0.125
K-273	0.07 × 0.03
K-878	0.25
2500	0.075 × 0.25

porosity of ~32% with an average pore size of 0.05 × 0.125 μm.

A knowledge of the area-specific resistivity of the separator saturated with the electrolyte, is important for battery design, especially those for high power applications. The voltage loss,  $\Delta E$ , in a battery on load is given by

$$\Delta E = E_{OCV} - E_{load} \quad (16)$$

$$= \Delta E_{ohmic} + \Delta E_{other},$$

$$\Delta E_{ohmic} = iR_{cell}. \quad (17)$$

Since  $R_{cell}$ , as shown in equation (15), primarily comes from the resistivity of the separator saturated

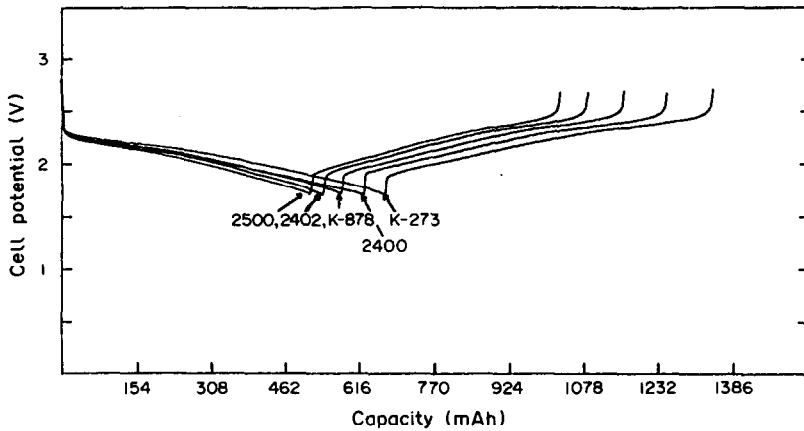


Fig. 2. A comparison of the cycles of AA size Li/TiS<sub>2</sub> cells containing different separators.  $I_d = 4 \text{ mA cm}^{-2}$ ,  $I_c = 0.5 \text{ mA cm}^{-2}$ .

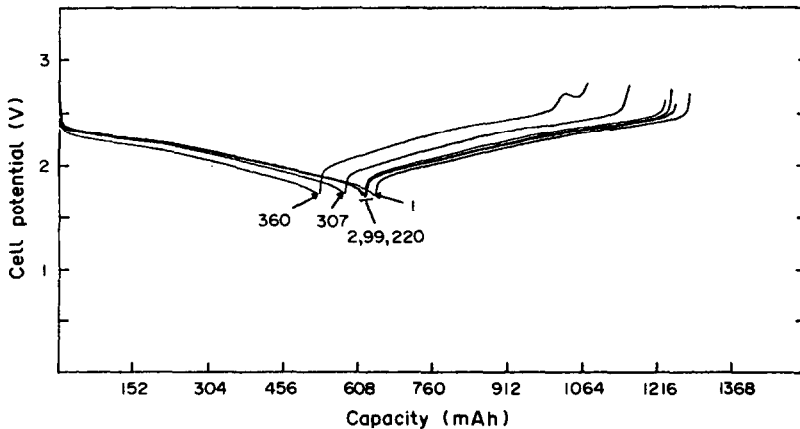


Fig. 3. Typical cycles of a AA size Li/TiS<sub>2</sub> cell utilizing Celgard 2400.  $I_d = 1.4 \text{ mA cm}^{-2}$ ;  $I_c = 0.7 \text{ mA cm}^{-2}$ .

with the electrolyte,

$$\Delta E_{\text{ohmic}} = \frac{i\rho_{\text{ms}}}{A}. \quad (18)$$

The limiting current  $I_1$  in a Li battery is largely determined by the porosity and tortuosity of the separator membrane. The limiting current, according to Atlung[35], is given by

$$I_1 = \frac{2FCD}{l(1-t_+)}. \quad (19)$$

In equation (19),  $C$  is the concentration of the Li ions,  $D$  is its diffusion coefficient,  $t_+$  is its transport number and  $l$  is the distance between the electrodes. When the separator porosity ( $P$ ) and tortuosity ( $T$ ) are factored in, equation (19) becomes

$$I_1 = \frac{2FCDP}{Tl(1-t_+)}. \quad (20)$$

It can be seen from equation (20) that the limiting current can be increased by increasing the porosity of the separator and decreasing its thickness and tortuosity. An experimental observation of this effect is depicted in Fig. 4 which depicts the discharge curves at 50 and 75 mA cm<sup>-2</sup> for Li/LiCoO<sub>2</sub> cells containing thin LiCoO<sub>2</sub> cathodes and three different separators. In addition to Celgard 2400 and K-273, Celgard K-292 was used. The latter is a biaxially stretched microporous membrane with a porosity of 55% and an average pore size of 0.38 μm. Each cell was charged, firstly to 4.3 V before being discharged. The best performance was obtained in cells containing K-292.

The safety of a rechargeable Li cell may be increased with the use of "shutdown" separators[32]. Its formation involves the application of waxes or composite structures containing a low-melting point polymer component in non-woven or membrane form. The low melting structure in the membrane

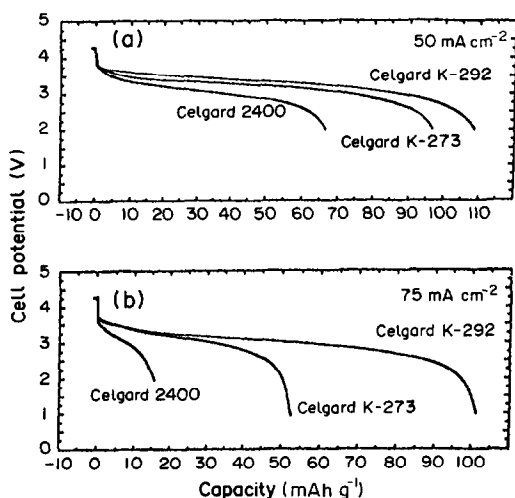


Fig. 4. Comparison of discharge curves for Li/LiCoO<sub>2</sub> cells with 2 mil cathodes and Celgard® 2400, Celgard K-273 or Celgard K-292 separator discharged at: (a) 50 mA cm<sup>-2</sup>; and (b) 75 mA cm<sup>-2</sup>. The electrolyte is 2.5 M LiAsF<sub>6</sub> in 75 v/o methyl acetate and 25 v/o PC.

will fuse as the cell temperature increases, for example, from an external short, and that, in turn, will cause a large increase in the resistance of the cell followed by its shut down. Separators claimed to have "shutdown" properties include a multiply sheet product in which one ply transforms to a non-porous structure at elevated temperatures[36], a thermal fuse with wax-coated fibers[37] and Celgard membranes with selected fusible materials in a pre-determined geometric array[32]. By choosing the fusible materials according to melting points, the shutdown temperatures can be tailored to suit the application. The ideal "shutdown separator" for a rechargeable Li cell would be one in which the fusible material melts at about 120°C while the principal separator membrane remains intact until after the melting point of Li. Such a separator will prevent the cell from internal short circuit even after the melting of the fusible material. The thermal excursions in a cell that is not internally shorted would be easier to manage.

### ALTERNATIVE ANODES

The limited rechargeability and the safety hazards of Li anode batteries can be overcome with the use of a material with lower Li activity for the anode than Li metal. The lower activity will greatly reduce the risk of passivation of the anode, and increase cell safety because of reduced reactivity with the electrolyte.

Alternative anodes comprise two classes of materials: (a) Li insertion compounds; and (b) Li alloys. They must possess several key properties.

- A low equivalent weight.
- A small free energy change for the insertion reaction with Li.
- A high diffusivity for Li<sup>+</sup> in the solid-state structure of the anode.
- High reversibility for the insertion reaction.
- Good electronic conductivity.
- Thermal stability and chemical compatibility with the electrolyte.
- Ease of fabrication into suitable electrode structures.

Materials which have been investigated include the Li insertion materials Li<sub>x</sub>Fe<sub>2</sub>O<sub>3</sub>, Li<sub>x</sub>WO<sub>2</sub> and graphitic carbon, alloys such as β-LiAl, δ-LiAl, LiCdPb, LiSnCd, LiAlMn and composite anodes such as Li/Li<sub>3</sub>N and Li<sub>x</sub>Pb-polyparaphenylene[15, 38]. Alternative anode cells demonstrated include LiAl/TiS<sub>2</sub>[39]WO<sub>2</sub>/Li<sub>x</sub>CoO<sub>2</sub>[40, 41], C/Li<sub>x</sub>NiO<sub>2</sub>[42], Li<sub>x</sub>Fe<sub>2</sub>O<sub>3</sub>/TiS<sub>2</sub>[38], C/Li<sub>x</sub>Mn<sub>2</sub>O<sub>4</sub>[43] and C/Li<sub>x</sub>CoO<sub>2</sub>[11].

These batteries without metallic Li have been called "Li ion" batteries. Two limitations of alternative anodes compared with Li metal are higher equivalent weights, and lower voltages for cells containing them. However, these disadvantages may in part be compensated for with the use of high voltage (~4 V vs. Li<sup>+</sup>/Li) cathodes such as Li<sub>x</sub>CoO<sub>2</sub>, Li<sub>x</sub>NiO<sub>2</sub> and Li<sub>x</sub>Mn<sub>2</sub>O<sub>4</sub>. Also, since lithiated carbon is air sensitive, high voltage cathodes are required to



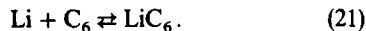
provide a Li ion source which is stable in the dry room oxygen atmosphere. The carbon anode is incorporated in the cell in the fully discharged form and Li is supplied through the cathode.

The performance of the  $\text{Li}_x\text{CoO}_2$  cathode is especially noteworthy. Its high-rate capability is exemplified by the data presented earlier in Fig. 4. The excellent rechargeability of  $\text{LiCoO}_2$  is demonstrated by the cycling data in Fig. 5 we have obtained recently for a  $\text{Li}/\text{LiCoO}_2$  cell.

Carbon was proposed as an insertion anode material as early as 1973[44]. However, recent interest in this material has been aroused by the Sony rechargeable  $\text{C}/\text{LiCoO}_2$  cell[11] apparently capable of greater than 1000 full depth of discharge cycles. Typical cycles for a Sony cell we obtained at different discharge/charge rates are presented in Fig. 6. At the low  $\text{C}/40$  rate the cell has an energy density of  $210 \text{ Wh l}^{-1}$  and a specific energy of  $88 \text{ Wh kg}^{-1}$ .

Energy densities significantly higher than those shown by the Sony cell should be possible with the use of improved carbon anodes. It is believed that

graphite has a theoretical intercalation capacity of 1 Li per  $\text{C}_6$ , equation (21).



This corresponds to a specific capacity of  $372 \text{ mAh g}^{-1}$ . If this capacity can be fully accessed, rechargeable  $\text{C}/\text{LiCoO}_2$  cells would be possible with specific energies between  $100\text{--}150 \text{ Wh kg}^{-1}$  and energy densities between  $250\text{--}400 \text{ Wh l}^{-1}$ . A variety of properties apparently affect the reversible Li intercalation efficiency of carbon. These include surface area, true density, crystallinity and the nature of surface groups. Fong *et al.*[45] found some irreversible reactions during the first cycle of Li/petroleum coke cells using  $\text{PC}/\text{LiAsF}_6$  as the electrolyte. Subsequent to the first cycle, the cell exhibited excellent reversibility. Our own experience is that the degree of crystallinity of the carbon is extremely important for high capacity and rechargeability. Many of the highly crystalline graphites we have examined did not cycle Li well. They promote electrolyte reduction, the extent of which seems to be a function

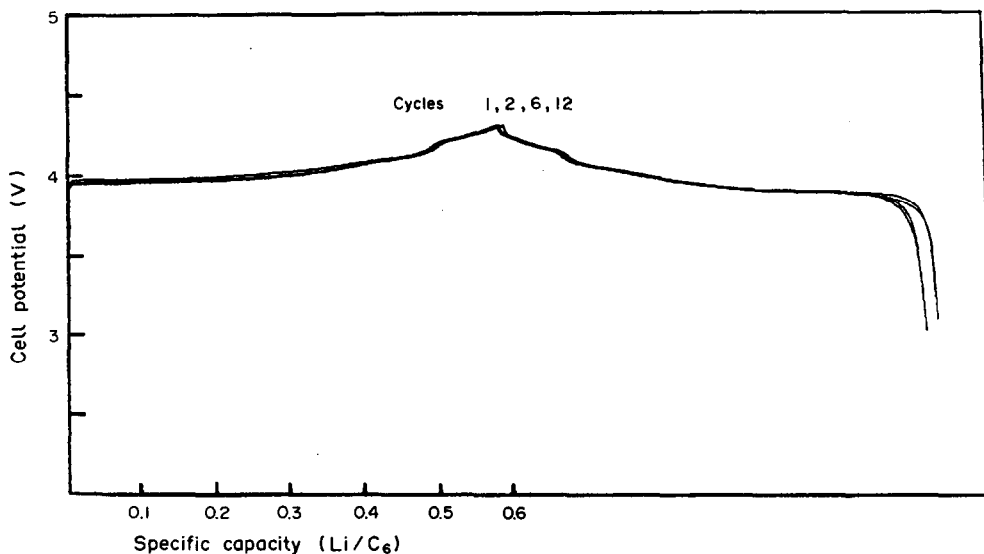


Fig. 5. Cycles of a  $\text{Li}/\text{LiCoO}_2$  cell at  $1 \text{ mA cm}^{-2}$ . The electrolyte is the same as that for the cells in Fig. 4.

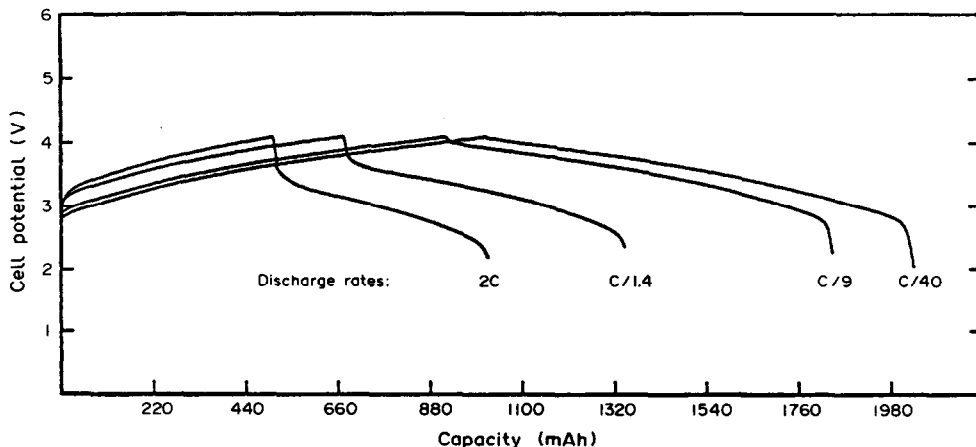


Fig. 6. Cycles of a Sony Li ion cell at room temperature.

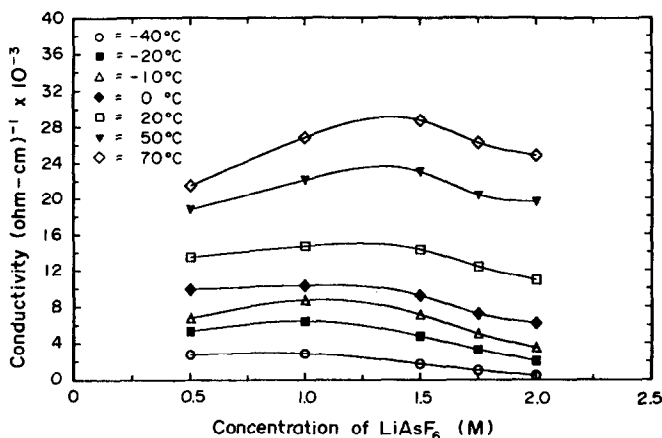


Fig. 7. Conductivities of electrolytes containing 50 v/o PC:50 v/o MA-LiAsF<sub>6</sub> at various concentrations as a function of temperature.

of the particle size of graphite. In our hands, the best performance was for a material with intermediate crystallinity resembling that of many petroleum cokes and the highest capacity we have obtained to date is  $\sim 200 \text{ mAh g}^{-1}$ . Capacities greater than  $300 \text{ mAh g}^{-1}$  have been reported recently by the Sony group[46] and their work also reinforces the effect of crystallinity of carbon on reversible Li cycling without interference from solvent reduction. Certainly, a significant amount of work remains to be done in the development of a carbon anode which exhibits high capacity along with long cycle life for the Li intercalation/deintercalation processes.

### ELECTROLYTES STABLE TO HIGH VOLTAGE CATHODES

The emergence of the high voltage cathodes, especially those with 4–4.5 V vs.  $\text{Li}^+/\text{Li}$ , necessitates the identification of electrolytes that are oxidatively stable in contact with them at the potentials required for the charge of the cells. The development of electrolytes with thermodynamic and/or kinetic stability for use in these batteries is therefore a major challenge.

Ether based electrolytes traditionally used in Li

anode batteries undergo oxidation, in some cases (*eg* THF) with polymerization, at potentials of about 4 V[47]. Most polyether based polymer electrolytes have also shown oxidation reactions between 4.0 and 4.5 V[48]. The oxidation reactions apparently involve the removal of an electron from the ether oxygen of the solvent followed by the degradation of the solvent.

The oxidative stability of non-aqueous solvents increases with the incorporation of certain electronegative groups such as nitrile ( $\text{CN}^-$ ), carbonate ( $\text{CO}_3^{2-}$ ) and esters ( $\text{RCOO}^-$ ). The CN group, with a bond energy of about  $930 \text{ kJ mol}^{-1}$ , is very resistant to oxidation. This is the reason why  $\text{CH}_3\text{CN}$  is the most ubiquitous solvent for electrochemical measurements, especially for reactions involving high oxidation potentials. For example, the polymerization of polythiophene is carried out at about 4.8 V in acetonitrile[49]. Unfortunately acetonitrile is unstable in contact with Li and cannot be used in Li anode batteries. Whether or not this solvent can be used in Li ion batteries remains to be established. The organic esters such as EC, PC and methyl formate (MF) have higher anodic stability than the ethers[47], and esters are traditionally the solvents of choice for use in the high voltage cathodes.

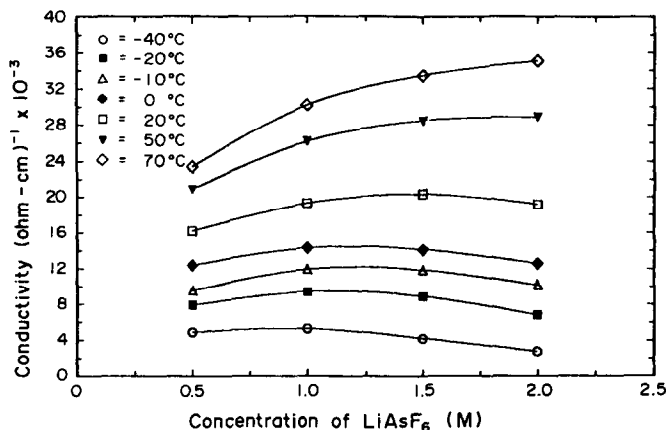


Fig. 8. Conductivities of electrolytes containing 25 v/o PC:75 v/o MA-LiAsF<sub>6</sub> at various concentrations as a function of temperature.

Indeed, the solvent used in the Sony cell appears to be primarily PC, while MF has been used by the Honeywell group in the Li/LiCoO<sub>2</sub> cell[28].

The Li/LiCoO<sub>2</sub> cell data shown in Figs 4 and 5 were obtained with the use of an electrolyte composed of 2M LiAsF<sub>6</sub> dissolved in a 3:1 by volume mixture of methyl acetate (MA) and PC. We have found that mixed electrolytes based on PC and MA have high conductivities (Figs 7 and 8) and an anodic stability to about 4.6 V vs. Li<sup>+</sup>/Li. It should be noted that the reduction properties of this solvent mixture have not yet been investigated, which would be important for its use in the Li ion batteries. Electrolytes with high anodic stability and good conductivity over a wide temperature range can also be prepared from solvent mixtures such as EC/MA or EC/PC/MA. Other low viscosity solvents with high anodic stability include methyl carbonate and ethyl carbonate.

Fundamental investigations are required to characterize the oxidation reactions of generic solvent based electrolytes and to identify electrolytes that are suitable for the development of "Li ion" batteries employing high voltage cathodes. It should be noted that when developing such electrolytes consideration should also be given to the redox stability of the Li salts. In this connection the work of Ciemiecki and Auburn[49] is noteworthy. They found the order of Li salt stability toward electrochemical oxidation to be LiClO<sub>4</sub> > LiAsF<sub>6</sub>, LiPF<sub>6</sub>, LiBF<sub>4</sub> > LiCF<sub>3</sub>SO<sub>3</sub> > LiAlCl<sub>4</sub>.

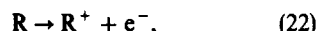
### OVERCHARGE AND OVERDISCHARGE PROTECTION OF SECONDARY LITHIUM BATTERIES

#### Overcharge protection

Many applications of secondary Li batteries require high voltage power sources which necessitate the fabrication of batteries of series-connected cells. A built-in mechanism to prevent overcharge of individual cells is a requirement for such batteries in order to maintain capacity balance among the individual cells as well as to prevent oxidative degradation of the electrolyte. In a recent paper we have discussed the principles underlying overcharge protection of secondary Li batteries[50, 51].

A highly desirable way to achieve overcharge protection is to use a chemical redox shuttle. This reagent added to the electrolyte would be unreactive until an overcharge situation arises. Once a potential above the normal charge cutoff voltage of the cell is reached, the redox shuttle would be activated. The

additive would be oxidized to products at the positive electrode [equation (22)].



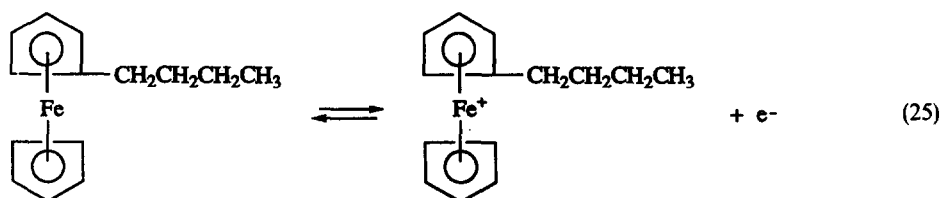
The oxidized products would diffuse to the negative electrode where it would either be electrochemically reduced or would react with Li to regenerate the starting material [equations (23) and (24)]. The cyclic nature of the conversion would maintain the cell potential "locked" at the oxidation potential of the redox reagent until termination of the charging.

Ideally, this material would have the following properties: good solubility in the electrolyte; an oxidation potential slightly higher than the normal charge limit of the cell but lower than the oxidation potential of the electrolyte; the ability to reduce its oxidized form at the anode without side reactions, and chemical stability in the cell of both the oxidized and reduced forms of the shuttle reagent.

EIC Laboratories, Inc. has been awarded U.S. and Foreign Patents for the discovery of metallocenes as a desirable class of overcharge protection redox additives for secondary Li batteries[51]. A prominent member of this class of reagents is *n*-butylferrocene. The redox reaction involving *n*-butylferrocene is shown in equation (25).

From cyclic voltammograms on a glassy carbon electrode in THF:2Me-THF/LiAsF<sub>6</sub> (1 M), a diffusion coefficient of  $2.2 \times 10^{-7} \text{ cm}^2 \text{ s}^{-1}$  for *n*-butylferrocene was calculated[51]. Assuming complete reversibility and diffusion controlled conditions, the limiting current for a solution containing 0.5 M *n*-butylferrocene is predicted to be  $1.4 \text{ mA cm}^{-2}$  ( $\sim 350 \text{ mA}$  in our 2 Ah cells[1]). Successive cycling of this 2 Ah cell with overcharge protection has been demonstrated[51]. *n*-Butylferrocene appeared to have little deleterious effect on the cycling efficiency of the Li electrode. The choice of *n*-butylferrocene out of the various metallocenes for use in combination with our standard electrolyte was made from considerations of the cell's discharge rate capability over a wide range of temperature and cycle life. One or more of other metallocenes[51] may be suitable for a different secondary Li cell.

The low diffusion rates of ferrocenes in non-aqueous solvents are an impediment to the use of these materials in cells requiring high-rate charging. Consequently, the identification of materials with redox and chemical stability properties similar to those of the ferrocenes and diffusion coefficients approaching that of Li<sup>+</sup> is highly desirable.



### Overdischarge protection

It is also necessary to protect individual cells of a battery from overdischarge to potentials below the cutoff voltage employed in the cycling of single cells. However, the redox shuttle concept applicable to overcharge protection is not readily applicable for overdischarge protection. This is because during overdischarge of a cathode-limited Li cell the anode (except under voltage reversal) is situated at a lower potential than the cathode. Consequently, the material reduced at the cathode cannot be oxidized at the anode. (The voltage reversal condition represents an extreme case of overdischarge and a cell encountering this condition will, most probably subsequently not function.) Among alternative concepts which deserve attention are: the inclusion to the cathode of a small amount of a second reversible material with a lower discharge potential than that of the principal cathode material; and the use of a second material in the cathode that can act as a chemical diode and shut down the discharge reaction when the potential falls below a certain value.

## POLYMER ELECTROLYTES AND SOLID-STATE BATTERIES

Polymer electrolyte based batteries are actively being developed because of the advantages they offer in comparison to conventional systems containing liquid electrolytes. For example, polymer electrolyte batteries can be inexpensively manufactured from structural units composed of anode, cathode and electrolyte laminates. Laminate based construction allows all solid-state modular battery fabrication in a variety of sizes and shapes including spirally wound, rectangular and Z folded geometries. Applications such as cellular telephones and smart credit cards require thin flat batteries which are readily fabricated from polymer electrolyte based systems. Another attractive feature of polymer electrolyte batteries is that they can be designed in the bipolar configuration without the intercell leakage current and the associated self-discharge problems encountered in liquid electrolyte systems. The bipolar design embodies a significant reduction in the hardware weight of the battery and translates into higher energy and power densities than monopolar systems. Also, the intercell impedance in a bipolar battery is independent of the size of the battery, thereby allowing higher power densities than monopolar batteries.

The technical impediment to the development of room temperature polymer electrolyte batteries has been the identification of a suitable electrolyte. Polymer electrolytes for such batteries must possess many desirable properties. These include:

- a conductivity between  $10^{-4}$  and  $10^{-3} \text{ S cm}^{-1}$  in the ambient temperature range of  $-40$  to  $70^\circ\text{C}$ ;
- good dimensional stability in the  $-40$  to  $70^\circ\text{C}$  range;
- good thermal stability in the  $-40$  to  $70^\circ\text{C}$  range;
- an electrochemical stability window spanning the potentials between  $0.0$  and  $\geq 4.0 \text{ V}$  vs.  $\text{Li}^+/\text{Li}$ ;

- chemical compatibility with both the Li anode and the cathode over the whole ambient temperature range; and
- an ability to afford Li cycling (recharge) at an efficiency of greater than 99%.

While high room temperature conductivity is of paramount importance, the conductivity must be complemented by good dimensional stability since the polymer electrolyte also functions as a separator in the battery providing electrical insulation between the anode and cathode. That means that it must be possible to process the electrolyte into free-standing thin films having adequate mechanical strength for withstanding the physical dynamics of the electrodes during cycling of secondary Li batteries. In this respect, the mechanical strength of polymer electrolytes should be comparable to that of conventional, non-aqueous liquid electrolyte battery separators such as porous polyethylene and polypropylene membranes having typical thicknesses of  $0.0025$ – $0.005 \text{ cm}$ . On the other hand, to expect an ionic conductivity similar to that of highly conductive liquid electrolytes and a dimensional stability reminiscent of solids in the same polymer electrolyte is to expect the coexistence of two properties which are probably mutually exclusive, especially in view of the fact that the mechanism by which ions are transported in polymer electrolytes is not significantly different from that involved in liquid electrolytes. Indeed, it has been necessary to pursue unusual approaches in order to develop polymer electrolytes having room temperature conductivities of the order of  $10^{-3} \text{ ohm}^{-1} \text{ cm}^{-1}$ .

Conventional polymer electrolytes are complexes of Li salts with polymers having electron donor groups. The classical examples are Li salt complexes of poly(ethylene oxide) PEO and poly(propylene oxide), PPO[48]. These polymers are low dielectric materials and, in consequence, lithium salts having complex anions such as  $\text{LiAsF}_6$ ,  $\text{LiBF}_4$ ,  $\text{LiClO}_4$  and  $\text{LiCF}_3\text{SO}_3$  which have low lattice energies give rise to better conductivity than salts such as  $\text{LiCl}$  and  $\text{LiBr}$  which have high lattice energies. In fact, the general principles which apply to the conductivity mechanism in liquid electrolytes are largely applicable to solid polymer electrolytes. Theoretical aspects of ionic conductivity in solid polymer electrolytes have been described[52].

The low conductivity usually observed in a conventional solid polymer electrolytes at room temperature is predominantly the result of the low mobility of the ions. We may illustrate this with the conductivities of Li salt complexes of poly(ethylene oxide) (PEO) and Li salt solutions in diethyl ether (DEE). The dielectric constants of PEO and DEE are very similar, being  $\sim 5$  and  $4.3$ , respectively. Consequently, the number of charge carriers for a given Li salt concentration are expected to be of the same magnitude in both electrolytes. However,  $(\text{PEO})_8\text{LiX}$  have room temperature conductivities of only about  $10^{-9} \text{ ohm}^{-1} \text{ cm}^{-1}$  whereas DEE/LiX solutions have conductivities of about  $10^{-3} \text{ ohm}^{-1} \text{ cm}^{-1}$ . Clearly, the higher conductivity of the latter solutions is due to the higher mobility of the ions.

Because of the similarity in the conductivity mechanism of polymer and organic liquid electrolytes, the maximum conductivity that can be obtained at room temperature from an electrolyte based on conventional polymer hosts can be gleaned from an examination of the conductivities of some liquid electrolytes. Table 7 lists the conductivities of LiAsF<sub>6</sub> (1 M) in four different solvents. LiAsF<sub>6</sub> is a relatively low lattice energy salt with a lattice energy that is apparently lower than that of LiClO<sub>4</sub> and LiBF<sub>4</sub> and it forms highly conductive solutions in organic solvents. An examination of the conductivity data in Table 7 reveals that the conductivity is a strong function of the viscosity of the solvent. Based on the dielectric constants of the solvents alone conductivity should follow the order PC > SL > AN > THF. However, the data in Table 7 correlate inversely with solvent viscosity. Only when the viscosities are similar, as in THF and AN, does the higher permittivity AN produce solutions of higher conductivity than the lower permittivity THF. It can be said that for highly concentrated organic electrolyte solutions, such as those used in non-aqueous Li batteries, the conductivity for a given Li salt correlates fairly with the inverse of the solution viscosity when the solvents do not differ significantly in dielectric constants. Note that the conductivity of SL/1 M LiAsF<sub>6</sub> at 25°C is only  $2.7 \times 10^{-3} \text{ S cm}^{-1}$ . Given the similarities in the conductivity mechanisms of liquid and polymer electrolytes and the fact that solid polymer electrolytes comprise much more viscous media than liquid electrolytes, a conductivity of about  $10^{-4} \text{ S cm}^{-1}$  at room temperature may represent the maximum that can be achieved in conventional polymer electrolytes. A discussion of conventional polymer electrolytes with high conductivities has been given recently [12, 14].

Non-conventional polymer electrolytes with con-

ductivities of  $\geq 10^{-3} \text{ ohm}^{-1} \text{ cm}^{-1}$  at room temperature can be obtained by immobilizing Li salt-solvates of high dielectric solvents in a polymer network [12, 14]. Examples of such electrolytes are those containing Li salt-solvates of a mixture of propylene carbonate and ethylene carbonate incorporated in a polymer network of either polyacrylonitrile (PAN), poly(vinyl pyrrolidinone) (PVP) or poly(ethylene glycol diacrylate), PEGDA [14].

A comparison of the conductivities of some of these non-conventional electrolytes (Nos 1-5) with those of some conventional polymer electrolytes (Nos 7 and 8) is given in Table 8. The Li salts used are LiClO<sub>4</sub>, LiAsF<sub>6</sub>, LiCF<sub>3</sub>SO<sub>3</sub>, LiPF<sub>6</sub> and LiN(SO<sub>2</sub>CF<sub>3</sub>)<sub>2</sub>. Compared to polymer electrolytes derived from the long chain polymers of poly(ethylene oxide), PEO and poly[bis-(methoxyethoxy)ethoxy]phosphazene, MEEP, the PAN based electrolytes have two-six orders of magnitude higher conductivity at room temperature.

PAN based electrolytes have demonstrated good electrochemical stability in the potential range of 0-5 V vs. Li<sup>+</sup>/Li. Evidence for their exceptional electrochemical and chemical stability is provided by the performance of solid-state Li and C anode cells. These cells have been fabricated from a laminate of the electrolyte being sandwiched by an anode and a cathode laminate. The cathode is either a 3 or 4 V lithiated manganese dioxide, formulated as LiMn<sub>2</sub>O<sub>4</sub>. The capacity utilization of Li/LiMn<sub>2</sub>O<sub>4</sub> cells at various rates at 70, 50, 25, 0 and -20°C, and cycling performance of 3 and 4 V Li/LiMn<sub>2</sub>O<sub>4</sub> cells and a 3.5 V C/LiMn<sub>2</sub>O<sub>4</sub> cell are presented in Figs 9-15. More than 200 full depth-of-discharge cycles have been achieved in a Li/LiMn<sub>2</sub>O<sub>4</sub> cell while the C/LiMn<sub>2</sub>O<sub>4</sub> cell exceeded 500 cycles. When fully developed the Li anode cell will have a specific energy > 120 Wh kg<sup>-1</sup> and the C/LiMn<sub>2</sub>O<sub>4</sub> cell will

Table 7. Conductivities of 1 molar LiAsF<sub>6</sub> solutions in some organic solvents

Solvent	Dielectric constant ( $\epsilon$ )	Viscosity (cP)	Donor numbers (DN)	Conductivity at 25°C (ohm <sup>-1</sup> cm <sup>-1</sup> )
Sulfolane (SL)	43.3 (30°C)	10.28 (30°C)	14.8	$2.7 \times 10^{-3}$
Propylene carbonate (PC)	64.4	2.53	15.1	$6.0 \times 10^{-3}$
Acetonitrile (AN)	39.9	0.34	14.1	$50 \times 10^{-3}$
Tetrahydrofuran (THF)	7.4	0.46	20.0	$14 \times 10^{-3}$

Table 8. Conductivities of PAN-based polymer electrolytes compared to PEO and MEEP based electrolytes at 20°C

Electrolyte number	Electrolytes*	Ionic conductivity at 20°C (ohm <sup>-1</sup> cm <sup>-1</sup> )
1	21 m/o PAN/38 EC/33 PC/8 m/o LiClO <sub>4</sub>	$1.7 \times 10^{-3}$
2	21 m/o PAN/38 EC/33 PC/8 m/o LiAsF <sub>6</sub>	$2 \times 10^{-3}$
3	21 m/o PAN/40 EC/34 PC/5 m/o LiCF <sub>3</sub> SO <sub>3</sub>	$2 \times 10^{-3}$
4	21 m/o PAN/41 EC/35 PC/3 m/o LiN(SO <sub>2</sub> CF <sub>3</sub> ) <sub>2</sub>	$2 \times 10^{-3}$
5	21 m/o PAN/41 EC/35 PC/3 m/o LiPF <sub>6</sub>	$1.4 \times 10^{-3}$
6	25 PVP/35 EC/30 PC/10 LiCF <sub>3</sub> SO <sub>3</sub>	$4.0 \times 10^{-4}$
7	MEEP-[LiN(CF <sub>3</sub> SO <sub>2</sub> ) <sub>2</sub> ] <sub>0.25</sub>	$6.5 \times 10^{-5}$
8	55 w/o MEEP/45 w/o PEO-[LiN(CF <sub>3</sub> SO <sub>2</sub> ) <sub>2</sub> ] <sub>0.13</sub>	$6.7 \times 10^{-5}$
9	PEO-(LiClO <sub>4</sub> ) <sub>0.13</sub>	$3.9 \times 10^{-9}$

\* m/o stands for mole per cent and w/o, weight per cent.

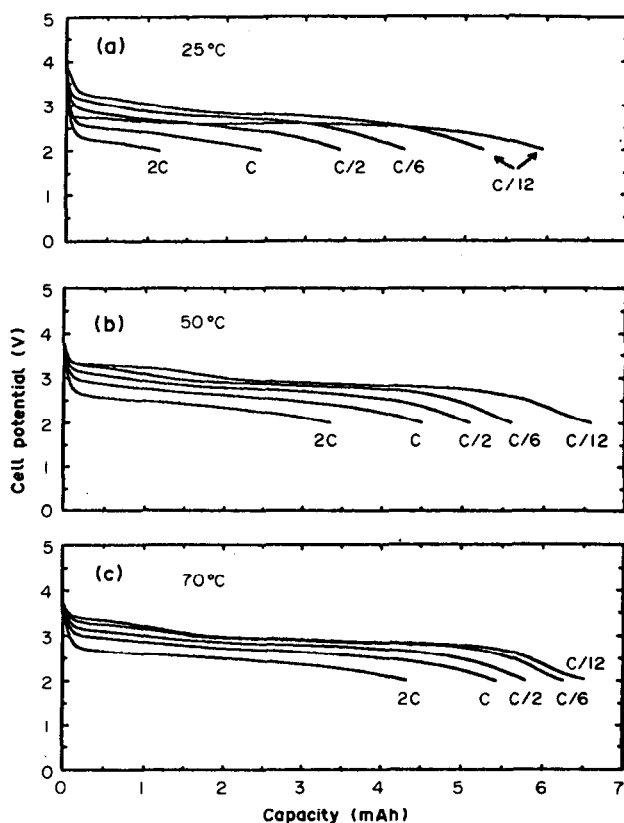
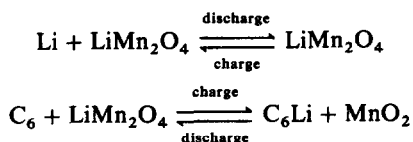


Fig. 9. Discharge curves for Li/PAN based electrolyte/LiMn<sub>2</sub>O<sub>4</sub> cell at different rates and temperatures. The six mAh capacity corresponds approximately to 0.5 Li per Mn.

have  $> 100 \text{ Wh kg}^{-1}$ . The idealized discharge/charge reactions are shown in equations (26) and (27)



The emergence of the non-conventional polymer electrolytes having high room temperature conductivity offers considerable flexibility in the design of solid-state batteries. However, the presence of a considerable amount of liquid in these electrolytes reminds us of the problems of reactions and passivation experienced by the Li anode in organic liquid electrolytes. Similar concerns in the polymer electro-

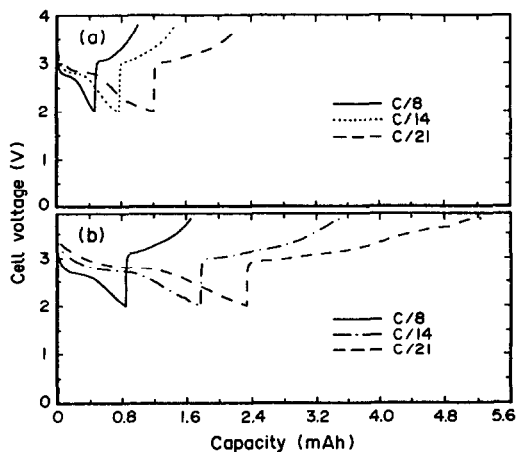


Fig. 10. Effect of electrolyte conductivity on the capacity of Li/LiMn<sub>2</sub>O<sub>4</sub> cells at 0°C. Theoretical capacity of cell is 3mAh: (a) PAN based electrolyte with lower conductivity ( $\sigma$  at  $-20^\circ\text{C}$ ,  $3 \times 10^{-4} \text{ ohm}^{-1} \text{ cm}^{-1}$ ); (b) electrolyte with higher conductivity ( $\sigma$  at  $-20^\circ\text{C}$ ,  $6 \times 10^{-4} \text{ ohm}^{-1} \text{ cm}^{-1}$ ).

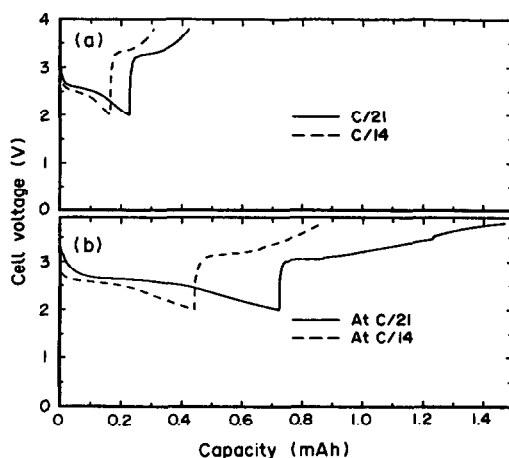


Fig. 11. Effect of electrolyte conductivity on the capacity of Li/LiMn<sub>2</sub>O<sub>4</sub> cells at  $-20^\circ\text{C}$ . Theoretical capacity of cell is 3mAh: (a) PAN based electrolyte with lower conductivity ( $\sigma$  at  $-20^\circ\text{C}$ ,  $3 \times 10^{-4} \text{ ohm}^{-1} \text{ cm}^{-1}$ ); (b) electrolyte with higher conductivity ( $\sigma$  at  $-20^\circ\text{C}$ ,  $6 \times 10^{-4} \text{ ohm}^{-1} \text{ cm}^{-1}$ ).

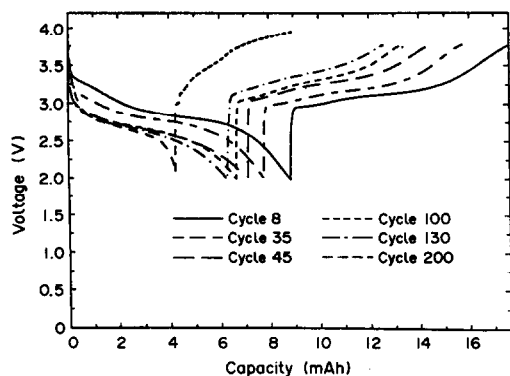


Fig. 12. The cycling behavior of a Li/LiMn<sub>2</sub>O<sub>4</sub> 3 V cell at room temperature containing PAN based solid electrolyte. Discharge at C/10 and charge at C/20.

lyte batteries are not totally unfounded. On the other hand, the ability to fabricate solid-state batteries with performance reminiscent of liquid electrolyte systems is a significant technological advantage. In order to further advance this technology, however, it is essential to have a good understanding of the properties of the Li/polymer electrolyte interface so that timely solutions can be found for problems of the types which prevented the commercialization of the liquid electrolyte-based rechargeable Li batteries. Our preliminary results of the studies of the Li/polymer electrolyte interface

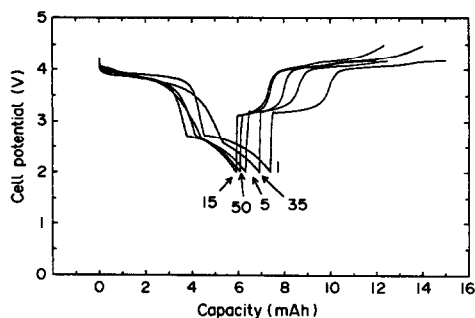


Fig. 13. The cycling behavior of a Li/Mn<sub>2</sub>O<sub>4</sub> 4 V solid-state cell at room temperature and the C/8 rate with a PAN based electrolyte.

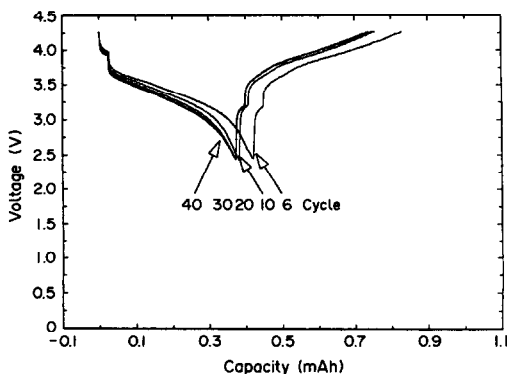


Fig. 14. The cycling behavior of a C/LiMn<sub>2</sub>O<sub>4</sub> solid-state cell at room temperature and the C/2 rate with a PAN-based electrolyte.

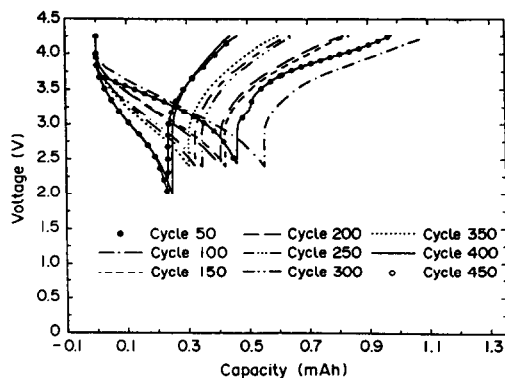


Fig. 15. The 50th and higher cycles of the C/LiMn<sub>2</sub>O<sub>4</sub> cell shown in the previous figure at the C/3 rate.

have been reported[53, 54]. For the immediate future Li ion solid-state batteries may be where the non-conventional polymer electrolytes will be used.

*Acknowledgements*—This article was written with financial support from the Department of Energy through Grant No. DF-FG01-90ER81078. The efforts of the colleagues M. Alamgir, D. M. Pasquariello and U. M. Twardoch are gratefully acknowledged.

## REFERENCES

1. K. M. Abraham, D. M. Pasquariello and D. A. Schwartz, *J. Power Sources* **26**, 247 (1989).
2. A. C. Makrides, K. M. Abraham, G. L. Holleck, T. H. Nguyen and R. J. Hurd, in *Proc. 34th Power Sources Symp.* p. 167. Pennington, New Jersey (1990).
3. J. Broadhead, *The Electrochemical Society Proceedings* Vol. PV87-16 (1987).
4. *JEC Battery Newsletter* p. 26. February (1988).
5. J. A. R. Stiles, in *Practical Lithium Batteries* (Edited by Y. Matsuda and C. R. Schlaikjer), p. 74. JEC Press, U.S.A. (1988).
6. Unpublished work at EIC Laboratories on 100 Ah Li/TiS<sub>2</sub> Cells.
7. K. M. Abraham, J. L. Goldman and F. J. Martin, in *Proc. 31st Power Sources Symp.* Cherry Hill, New Jersey (1984).
8. K. M. Abraham, P. B. Harris and D. L. Natwig, *J. electrochem. Soc.* **130**, 2309 (1983).
9. G. L. Holleck *et al.*, in *Proc. 30th Power Sources Symp.* p. 68. Atlantic City, New Jersey (1982).
10. M. Broussely, F. Pertion, J. Labat, R. J. Staniewicz and A. Romero, *Sixth International Meeting on Li Batteries, Münster, Germany*, Abstract No. Thu-02, p. 92 (1992).
11. T. Nagaura, "A Lithium Ion Battery", presented at the 4th International Rechargeable Battery Seminar, Deerfield Beach, Florida (1990).
12. K. M. Abraham, in *Applications of Electroactive Polymers* (Edited by B. Scrosati), Chap. 3. Chapman and Hall, London, 1993.
13. K. M. Abraham and M. Alamgir, *Chem. Mater.* **3**, 339 (1991).
14. K. M. Abraham and M. Alamgir, *J. electrochem. Soc.* **137**, 1657 (1990).
15. K. M. Abraham, *The Electrochemical Society Symposium Proceedings* Vol. PV90-5, p. 1 (1990) and references therein.
16. D. M. Pasquariello, K. M. Abraham, E. B. Willstaedt, D. H. Shen and S. Surampudi, *Fall Meeting of the Electrochemical Society, Toronto, Canada*, Abstract No. 46. October (1992).

17. K. M. Abraham, D. M. Pasquariello and F. J. Martin, *J. electrochem. Soc.* **133**, 643 (1986).
18. K. M. Abraham and S. B. Brummer, in *Lithium Batteries* (Edited by J. P. Gabano), Chap. 13. Academic Press, New York (1983), see also Chap. 2 in this book by G. Blomgren.
19. V. R. Koch, *J. electrochem. Soc.* **126**, 181 (1979).
20. J. R. Stiles, *New Mats New Procs* **3**, 89 (1985).
21. L. W. Brand, I. Chi, S. M. Granstaff and B. Vyas, U.S. Patent 4,753,859 (1988).
22. D. Shen, S. Subbarao, F. Deliganis and S. Dawson, in *Proc. 33rd Power Sources Symp. Cherry Hill, New Jersey*, p. 11 (1988).
23. G. H. Newman, R. W. Francis, L. H. Gaines and B. M. L. Rao, *J. electrochem. Soc.* **127**, 2025 (1980).
24. L. A. Dominey, V. R. Koch and T. J. Blakeley, *Electrochim. Acta* **37**, 1551 (1992).
25. D. P. Wilkinson, H. Blom, K. Brandt and D. Wainwright, *J. Power Sources* **36**, 517 (1991).
26. C. J. Post and E. S. Takeuchi, in *Proc. 35th Power Sources Symposium, Cherry Hill, New Jersey* (1992).
27. K. M. Abraham and D. M. Pasquariello, unpublished work.
28. W. B. Ebner, J. L. Simmons and D. L. Chua, in *Proc. 33rd International Power Sources Symp. Cherry Hill, New Jersey*, p. 11 (1988).
29. K. M. Abraham, *J. Power Sources* **14**, 179 (1985).
30. Y. Matsuda, M. Morita and A. Seiki, in *Proc. of the Symposium on Rechargeable Li Batteries* (Edited by S. Subbarao *et al.*), Vol. PV90-5, p. 67. The Electrochemical Society, Pennington, New Jersey (1990).
31. D. Shen *et al.*, in *Proc. of the Symposium on Rechargeable Li Batteries* (Edited by S. Subbarao *et al.*), Vol. PV90-5, p. 114. The Electrochemical Society, Pennington, New Jersey (1990).
32. D. K. Hoffman and K. M. Abraham, in *Proc. of the Fifth International Seminar on Lithium Battery Technology and Applications, Deerfield Beach, Florida* (1991).
33. R. B. MacMullin and G. A. Muccini, *J. AIChE*, **2**, 393 (1956).
34. K. M. Abraham and U. M. Twardoch, work carried out at EIC Laboratories in collaboration with D. K. Hoffman of Hoechst-Celanese, Charlotte, NC. Dr Twardoch derived equations (5)–(14) based on the work in [33].
35. S. Atlung, K. West and T. Jacobsen, *J. electrochem. Soc.* **126**, 1311 (1979).
36. J. T. Lundquist, C. B. Lundsager, N. I. Palmer and H. J. Troffkin, U.S. Patent 4,650,730 and U.S. Patent 4,731,304 (1987).
37. M. A. Faust, M. R. Suchauski and H. W. Osterhoudt, U.S. Patent 4,741,979 (1988).
38. K. M. Abraham, D. M. Pasquariello and E. B. Willstaedt, *J. electrochem. Soc.* **137**, 743 (1990) and references therein.
39. B. M. L. Rao, R. W. Francis and H. A. Christopher, *J. electrochem. Soc.* **124**, 1490 (1977).
40. B. Di Pietro, M. Patriarca and B. Scrosati, *J. Power Sources* **8**, 289 (1982).
41. J. J. Auborn and Y. L. Barberio, *J. electrochem. Soc.* **134**, 638 (1987).
42. J. R. Dahn, U. von Sacken, M. W. Juzkow and H. Al-Janaby, *J. electrochem. Soc.* **138**, 2207 (1991).
43. D. Guyomard and J. M. Tarascon, *J. electrochem. Soc.* **139**, 937 (1992).
44. M. B. Armand, *Fast Ion Transport in Solids* (Edited by W. Van Gool), p. 665. North Holland, Amsterdam (1973).
45. R. Fong, U. von Sacken and J. R. Dahn, *J. electrochem. Soc.* **137**, 2009 (1990).
46. H. Imoto, A. Omaru, H. Azuma and Y. Nishi, *Fall Meeting of the Electrochemical Society, Toronto, Canada*, Abstract No. 26 (1992).
47. G. Blomgren, in *Lithium Batteries* (Edited by J. P. Gabano), Chap. 2. Academic Press, New York (1983), see also Chapter 13 in this book.
48. M. Armand, in *Polymer Electrolyte Reviews—1* (Edited by J. R. MacCallum and C. A. Vincent), Chap. 1. Elsevier Applied Science, New York (1987).
49. K. T. Ciemiecki and J. J. Auborn, *Electrochemical Society Proceedings* (Edited by A. N. Day), Vol. PV84-1, p. 363 (1984).
50. K. M. Abraham, D. M. Pasquariello and E. B. Willstaedt, in *Proc. of the 33rd International Power Sources Symp. Cherry Hill, New Jersey*, p. 38 (1988).
51. K. M. Abraham, D. M. Pasquariello and E. B. Willstaedt, *J. electrochem. Soc.* **137**, 1856 (1990), see also U.S. Patent 4,857,423 and European Pat. 0319182.
52. M. A. Ratner and D. F. Shriver, *Mat. Bulletin* **14**, 39 (1989).
53. K. M. Abraham, M. Alamgir, G. S. Jones and L. L. Wu, *Fall ECS Meeting, Phoenix, Arizona*, Abstract No. 691. October (1991).
54. K. M. Abraham and M. Alamgir, *Sixth International Meeting on Lithium Batteries, Münster, Germany*. Abstract No. Thu-01. May (1992) (to be published in *J. Power Sources*).